

# A Hybrid Integrity Solution for Precision Landing and Guidance

Kenn L. Gold and Alison K. Brown

NAVSYS Corporation

## Abstract

NAVSYS Corporation has designed a hybrid integrity monitoring solution for precision approach and landing in a GPS environment degraded by RF interference. The integrity solution described in this paper leverages the capabilities of next generation digital spatial processing and ultra-tightly-coupled (UTC) GPS/inertial integrated military User Equipment (UE). The design includes a spatial environment integrity monitor, a GPS/inertial RAIM solution that allows detection of small error drift rates before the blended solution can be corrupted and an integrity monitoring function embedded within the Kinematic Carrier Phase Tracking (KCPT) algorithms which provides a level of confidence on the final KCPT solution. Simulation results showing the expected performance of some aspects of this multi-level integrity monitoring approach are presented. A design for an aircraft GPS/inertial digital spatial processing receiver, the HAGR-A, is also included. This receiver, which is based on the NAVSYS Software GPS Receiver, will be used as a test bed for implementation and testing of these integrity monitoring techniques

## Shipboard Relative GPS (SRGPS)

The Joint Precision Approach and Landing (JPALS) Shipboard Relative GPS Concept (SRGPS) is illustrated in Figure 1. The goal of the SRGPS program is to provide a GPS-based system capable of automatically landing an aircraft on a moving carrier under all sea and weather conditions considered feasible for shipboard landings. The presently utilized Aircraft Carrier Landing System (ACLS) is a radar-based system which was developed more than 30 years ago and has a number of limitations that make the system inadequate to meet present and future ship-based automatic landing system requirements. The goal of SRGPS is to monitor and control up to 100

aircraft simultaneously throughout a range of 200 nautical miles from the landing site<sup>1</sup>. Integrity monitoring is especially important for the last 20 nm of an approach, and accuracy requirements are 30 cm 3-D 95% of the time.

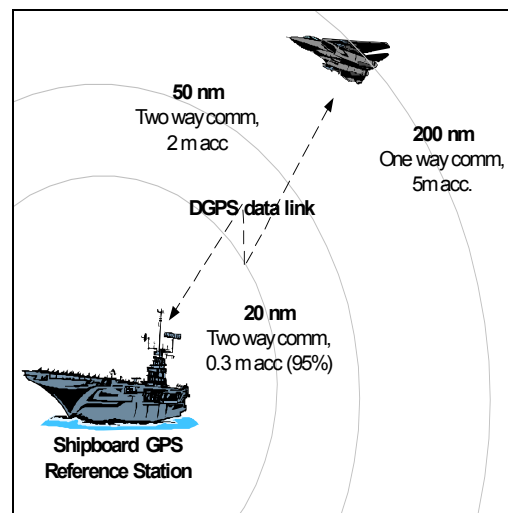


Figure 1 JPALS Shipboard Concept

The SRGPS architecture provides a precision approach and landing system capability for shipboard operations equivalent to local differential GPS systems used ashore, such as the FAA's Local Area Augmentation System (LAAS). A relative navigation approach is used for SRGPS with the "reference station" installed on a ship moving through the water and pitching, rolling, and yawing around its center of motion. In addition, the ship's touchdown point may translate up/down (heave), side to side (sway), and fore and aft (surge).

Since the shipboard landing environment is much more challenging than ashore, the SRGPS approach must use kinematic carrier phase tracking (KCPT) to achieve centimeter level positioning relative to the ship's touchdown point. Faulty measurements, even if detected prior to transmission, impact system performance. Therefore, improvements are

needed in the SRGPS shipboard reference station and signal processing to assure the continuity and integrity of the SRGPS corrections. Of particular concern are: (a) the robustness to signal blockages from the ship's superstructure; (b) the ability to operate in the presence of multipath while maintaining the carrier-phase and pseudo-range integrity; and (c) the ability to continue operation in the presence of radio frequency (RF) interference (from both normal ship operations and jammers) in a tactical environment.

### Next Generation High A/J Precision GPS User Equipment

Next generation GPS systems designed for JPALS and SRGPS operations are expected to have performance advantages over previous generation user equipment (UE). While these designs will meet the objective of high A/J, high accuracy performance, they must also implement integrity monitoring to be able to support precision approach and landing. Some of the elements of a high A/J aircraft receiver and the integrity monitoring components that must be addressed are illustrated in Figure 2. The shaded boxes in this figure highlight the areas of focus for the effort described in this paper.

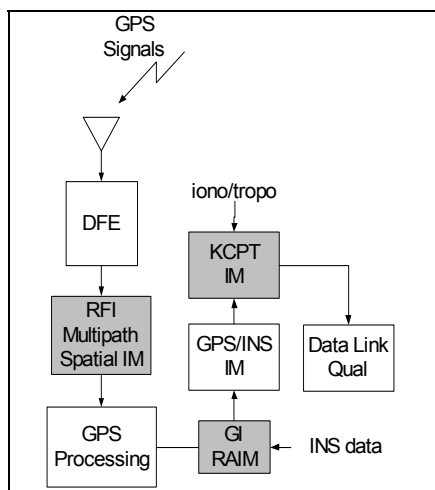


Figure 1 Integrity Monitoring Concept

### Overview of Integrity Monitoring Concerns

Spatial integrity monitoring must be addressed, and Digital Front End (DFE) failure is one area of concern. In a high A/J digital beam/null-

steering receiver, the RF signals from each antenna are first converted to an intermediate frequency (IF) signal and digitally sampled. The digital samples from the multiple antenna elements are then combined in the digital spatial processor to create the inputs to each channel of the GPS user equipment where the code and carrier correlation are performed.

One of the objectives of this design was to develop a Spatial Environment Estimator/Integrity Monitor to monitor for failure modes within the DFE and receiver spatial processing and also detect out-of-tolerance RF interference or multipath errors.

Inertial integration and Autonomous Integrity Monitoring (AIM) of the blended GPS/INS solution is another area of interest for the Hybrid Integrity monitoring solution. In previous coupled GPS/inertial systems, the outputs of the GPS tracking loops were fed to a GPS/inertial Kalman filter and autonomous integrity monitor (AIM). This technique was very effective in detecting GPS errors and meeting the integrity requirements for enroute and non-precision approach navigation<sup>ii</sup>.

Recently Ultra-Tightly Coupled (UTC) GPS/inertial integrated systems have been proposed that improve the ability to provide GPS updates under high jammer-to-signal (J/S) margins by coupling the inertial aiding into the receiver correlation channels<sup>iii</sup>. This complicates the integrity monitoring as the GPS observations are now coupled with inertial errors. Moreover, the integrity requirements for precision approach are more stringent than for previous applications. The proposed approach presented here is to implement a GPS/Inertial UTC RAIM algorithm to allow precise fault detection and exclusion of small range-rate errors. This approach allows validation of the UTC GPS observations before they are applied to the GPS/inertial Kalman filter. Additionally, Kalman down-dating is used to remove the effects of bad data from the filter.

To achieve the high level of accuracy needed to meet the JPALS and SRGPS performance requirements, kinematic carrier phase tracking

(KCPT) processing is used to compute the vehicle's position. This requires access to differential and kinematic corrections through the vehicle's data link and also requires knowledge of the local tropospheric and ionospheric corrections to be applied. Other groups are conducting research into robust means of assuring the integrity of the data link and atmospheric corrections. Another objective of this effort is to develop a robust KCPT integrity monitor that provides a positive indication of the validity of the KCPT precise positioning solution by assuring that correct integer ambiguity biases are selected.

### Spatial Environment Failure Modes

With the current generation analog controlled reception pattern antenna (CRPA) electronics in use by the DoD, a single composite RF signal is generated from the combined antenna inputs adapted to minimize any detected jammer signals. With next generation digital spatial processing GPS receiver designs, each antenna RF input is converted to a digital signal using a Digital Front-End. The DFE performs the function of phase-coherent down conversion and digitizing the received satellite RF signals. As illustrated in Figure 3, the DFE inputs from all of the antenna elements are then processed using spatial weights to create an optimized digital composite signal for each satellite tracking channel.

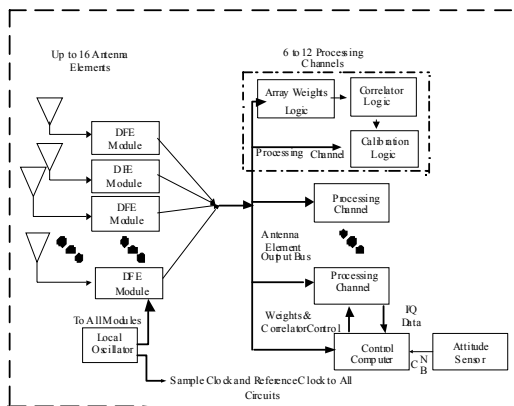


**Figure 3 GPS Spatial Signal Processing**

The weights are created digitally and constrained to avoid introducing any code or

carrier phase errors on the resulting combined signal<sup>iv</sup>.

### Spatial Environment Integrity Monitoring Approach

With conventional adaptive array processing, the combined signal is provided to the correlator channel for tracking. With digital beam/null-steering, the antenna patterns are optimized to minimize either the received jammer signal power or multipath signals, or both.

The spatial environment monitoring function is designed to monitor both pre-correlation and post-correlation spatial signal profiles. The post-correlation spatial signal profile. The pre-correlation power matrix is used to monitor for DFE failures, LO failures, and RF interference sources. The post-correlation power matrix and calibration signals provides an estimate of the multipath spatial profile and the residual errors following RFI suppression.

### Digital Front End Failure Detection

The operation of each individual DFE can be verified from monitoring the power of the cross-correlation terms relating to that element. If the DFE is operating correctly, then the diagonal elements of R should have the following relationship in equation 1.

$$\text{Eq. 1) } R_{ii} = N\sigma_n^2$$

By using a threshold test ( $R_{ii} < T$ ) this can identify a faulty DFE output. This element can be removed from the total composite solution by setting its weight  $w_i=0$ .

### Local Oscillator Failure

An LO failure will cause all of the DFE channels to cease operating. This can also be detected by monitoring the diagonal elements of the pre-correlation covariance matrix R.

### Satellite Signal Multipath

Multipath errors are caused by the satellite signals being received from reflected surfaces around the antenna array. This will distort the code and carrier tracking and introduce errors into the receiver. This failure mode can best be

detected through spatial processing to detect the angle of arrival of different multipath signals. The residual effect of the multipath on the signals after applying the digital weights can be estimated from the calibration signals using equation 2. This can also be used to provide a quality factor for the expected residual multipath errors on the receiver's code and carrier measurements.

$$\text{Eq. 2) } \underline{\varepsilon} = (\underline{e}_s \underline{w}') \underline{s}_c - \underline{e}_s \hat{S}(t)$$

### RF Interference

Although the effect of a GPS interference source can be mitigated using digital beam/null-steering, it can still degrade the accuracy of the GPS observations. High power continuous wave (CW) or pulsed signals can drive the DFE into saturation, suppressing the GPS signals. Broad-band noise jammers have the effect of decreasing the satellite observed carrier-to-noise ratio (C/N0) which in turn increases the pseudorange and carrier phase tracking errors<sup>v</sup>.

The post-correlation signal/noise can be estimated from knowledge of the pre-correlation covariance matrix, the applied beam/null-steering weights and the power spectral density of the jammer. The jammer/signal power is computed from equation 3, which comes from the Kaplan text.

$$\text{Eq. 3) } J_s = \frac{\underline{w}' R \underline{w}}{\underline{w}' \underline{e}_{S_i} \underline{e}_{S_i}' \underline{w}}$$

The post-correlation signal/noise ratio can then be computed as follows in equation 4. The scale factor Q=1 for a narrowband jammer and Q=2 for a broadband jammer.

$$\text{Eq. 4) } Cn0 = Pr - 10 * \log_{10} \left( kT + \frac{10^{(Js+Pr)/10}}{fQ} \right)$$

where

- Cn0 is the signal/noise in dB-Hz
- Pr is the nominal satellite power in dBw
- kT is the Boltzmann's constant scaled
- f is the chip spreading rate
- Q is the jammer scale factor

### GPS/Inertial Integrity Design

The purpose of the GPS/Inertial integrity design is to detect any out of tolerance GPS faults from the blended solution before they are applied. This is to prevent corrupted GPS data from propagating back into the GPS/Inertial solution. The GPS/Inertial Receiver Autonomous Integrity Monitor (GI-RAIM) algorithm design is described in the following sections. The purpose is to increase the J/S level to which GPS code and carrier observations can be made, while still providing a high integrity monitoring ability.

The proposed approach is to provide integrity monitoring on all updates provided to the inertial navigation Kalman filter. Unless the observations pass this high integrity test, they are not applied as measurement updates thus maintaining the integrity of the blended solution. The approach assumes that inertial systems will provide valid data over the short periods associated with final approach, or that the plane will be waved off.

Based on a previous study performed for AFRL/SN<sup>[vi]</sup>, a cascaded filter implementation is the best approach for maintaining the inertial navigation solution integrity. With the implementation shown in Figure , an optimal estimation technique is used to coherently combine the GPS signal from the C/A and P(Y) L1 and L2 broadcasts. By combining the I and Q data from the C/A, P(Y) L1 and P(Y) L2 into a single pre-filter, an optimal estimate for the pre-filter states (range, range rate, ionosphere, phase and amplitude) can be created to extract the best estimate of range and carrier-phase observations to apply to the GPS/inertial filter.

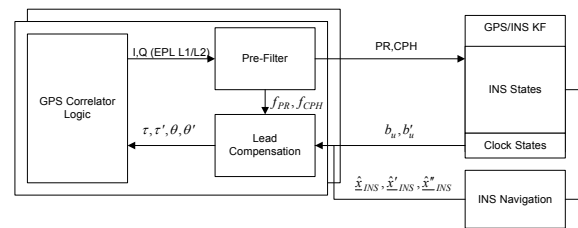


Figure 4 Cascaded GPS/Inertial Filter Approach

For each satellite tracked, this technique uses a total of 6 sets of observations (I and Q, Early,

Prompt and Late) for each of the codes correlated (C/A, P(Y) L1 and P(Y) L2) for each of the 20 msec accumulated samples, to estimate the pre-filter state estimates. This pre-filter solution is implemented based on a variant of an approach previously developed by The Aerospace Corporation<sup>[vii]</sup>.

### GPS/Inertial RAIM Algorithm

Before the observations generated by the UTC solution are used to update the GPS/inertial integrated Kalman filter, the observations are tested using the GI-RAIM algorithm. The GI-RAIM integrity algorithm is based on developing a set of conditional probabilities to assure detection of a satellite failure. This algorithm uses the “Bounded Probability of Missed Detection” (BPOD) approach developed by NAVSYS for the USCG<sup>[viii]</sup> and USAF<sup>[vi]</sup>.

The GI-RAIM algorithm steps are shown in Figure 5 and the principle of operation of the BPOD algorithm is illustrated in Figure . When a satellite failure occurs, the position and velocity error distribution has a mean offset with the locus of position or velocity errors distributed around this mean in an ellipse. The magnitude of the ellipse is determined by the satellite geometry and the random noise on the solution.

If it can be determined correctly which satellite has failed, it is possible to use the redundant information to estimate the magnitude of the failure on that satellite. From this information, the expected error distribution of that satellite can be predicted and the radial error ( $R_{PMD}$ ) can be computed such that  $(1-P_{MD})$  of the position solution loci can be expected to reside within this distribution.

Conversely, we can also compute the threshold Radial Position Error (R) for the Horizontal Alert Level (HAL),  $R_T$ . If  $R > R_T$ , then a satellite failure has occurred which would exceed the HAL. A similar approach can be used for detecting vertical errors that exceed the Vertical Alarm Limit (VAL).

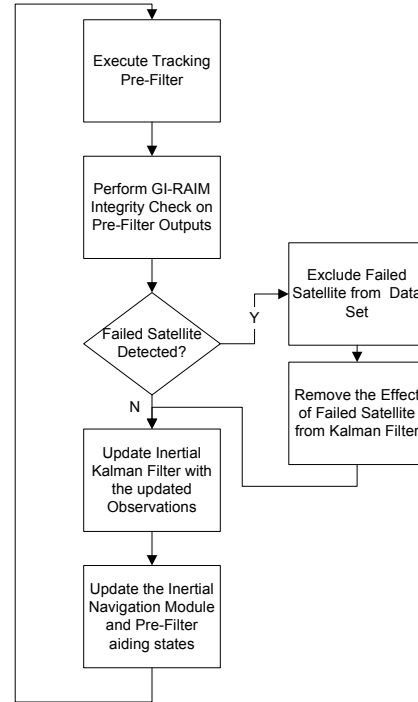


Figure 5 GI-RAIM Algorithm Steps

A major benefit of the BPOD algorithm is that it is independent of the measurement type and also will perform equally well in detecting errors in either the horizontal or vertical directions, simply by changing the geometric computations.

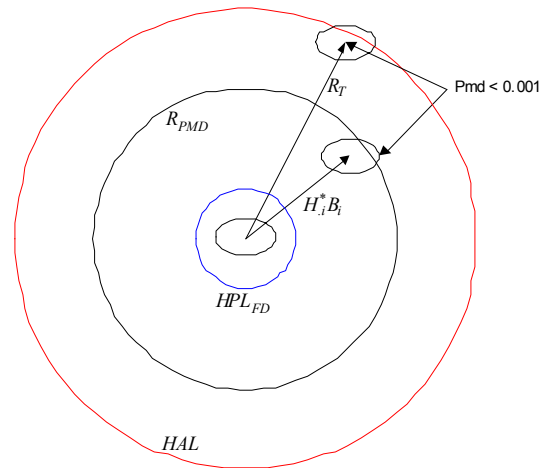


Figure 6 BPOD Principle of Operation

This means that the same algorithm can be applied to detect satellite failures that would cause the horizontal error to exceed the alert levels for en-route and non-precision approach phases of flight, and also to detect satellite

failures that would cause the vertical error to exceed the alert levels during a precision approach.

### GPS Fault Detection For Precision Approach

The proposed approach for GPS fault detection is to perform the GI-RAIM integrity test at a time interval given by  $dT$  seconds, prior to applying an update to the GPS/inertial Kalman filter solution. The inertial solution is then used to propagate the aircraft's position for the next  $dT$  seconds prior to another update being applied. The level of the integrity monitoring assumed for this study was:

- HAL: 1 meter
- VAL: 1 meter (goal)
- Probability of undetected error:  $10^{-7}$
- Continuity:  $10^4$
- Availability: 99.8+%

The inertial errors will grow during the time between GPS updates ( $dT$ ) due to drift rates and biases in the accelerometers and gyroscopes. Our model assumed an LN-100 inertial measurement system and the random position error growth, assuming no initial velocity error, is plotted in Figure 7 as a function of time to show the sensitivity to time. For the first few seconds, the position error growth is dominated by the velocity error. As the time increases though beyond 20 seconds, the inertial errors start to dominate. To assure that the position is within the HAL and VAL at time  $dT$  with the desired probability, the 1-sigma position error, without any velocity error component is computed from equation 5. HAL and VAL values are then computed from eq) 6 and 7..

### Eq. 5)

$$\sigma_p^2(dT) = E[P(t_0)^2] + B_a^2 dT^4 / 2^2 + G^2 B_{RW}^2 dT^5 / (2.5)^2 + G^2 B_G^2 dT^6 / 3^2$$

### Eq. 6) and Eq. 7).

$$\Pr ob(P_x^2(dT) + P_y^2(dT) < HAL^2) = \chi^2 \left( \frac{HAL^2}{\sigma_p^2(dT)} \middle| V_0 dT, 2 \right) = 1 - P_{MD}$$

$$\Pr ob(P_z^2(dT) < VAL^2) = \chi^2 \left( \frac{VAL^2}{\sigma_p^2(dT)} \middle| V_0 dT, 1 \right) = 1 - P_{MD}$$

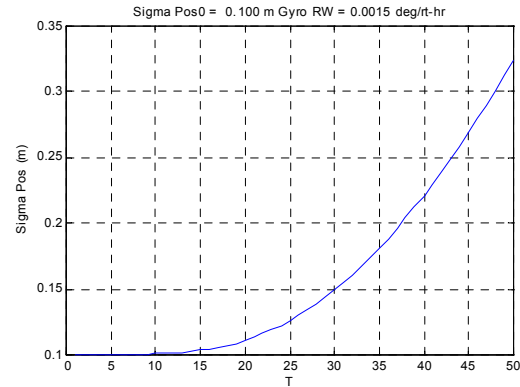


**Figure 7 Inertial Position Error Propagation with No Initial Velocity Error**

As the time interval increases, the range-rate observations become more accurate which in turn allows lower velocity errors to be trapped by the BPOD algorithm. However, as the time interval increases, the required velocity alarm limit that must be detected to assure that the position error remains within the HAL and VAL levels also decreases. The optimum time interval to perform the integrity test is calculated as a function of the integrity availability. That is, global integrity availability over a 24-hour period was computed for the current GPS satellite constellation and if the integrity geometry at any location and point in time was not sufficient to detect a failure on any GPS satellite in view to within the specified HAL and VAL limits then the integrity solution was considered unavailable. Preliminary simulation results show that to maintain 99.8% availability, HAL and VAL must be relaxed to 1.3 and 2.0 respectively.

### Velocity Error Failure Detection Simulation

In order to simulate the performance of the velocity error failure detection capability, a simulation program was written to verify that small range-rate errors were detected as expected using the BPOD algorithm to assure that failures would be observed before the alarm limits were exceeded.

Assuming an LN-100 inertial system with the error growth shown in Figure , the Velocity-Horizontal and Vertical Alarm Limits (V-HAL and V-VAL) that must be met to assure that the position HAL and VAL levels are met to the specified probabilities derived from equation 5 thru equation 7, are given below.

$$V\_Hal=0.072116 \text{ m/s}$$

$$V\_Val=0.072509 \text{ m/s}$$

The simulation modeled random carrier phase errors with a 1-sigma distribution of 2 cm. A bias range-rate error of 0.4 m/sec was then introduced onto each individual satellite signal in turn to determine whether the BPOD algorithm would correctly identify and reject this failure before the Velocity-HAL or VAL alarm limits were exceeded. The results of this simulation are shown in Figure 8 and Figure 9 for the horizontal and vertical velocity errors respectively. The Grey points mark satellite failures which were undetected by the BPOD algorithm. The Black points show satellites that were identified as failed and rejected from the solution by the BPOD algorithm. Since there are no cases of undetected failures outside of the HAL and VAL boundaries, these figures show that there were no cases of false misidentification or missed detections where the failure had caused either the horizontal or vertical alarm limits to be exceeded. Based on this analysis the BPOD algorithm appears to provide a robust method of identifying range-rate errors on the delta-range observations before they can corrupt the inertial navigation velocity solution sufficiently to exceed the precision approach limits.

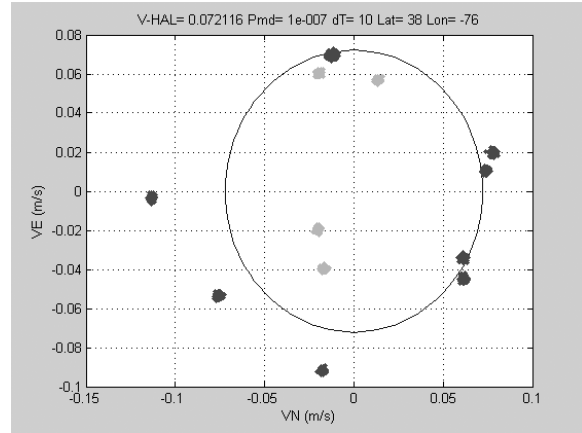


**Figure 8 Velocity Horizontal Alarm Limits for HAL=1.3, VAL=2.0 and dT=10 (Grey marks undetected satellite failures, Black marks detected satellite failures)**

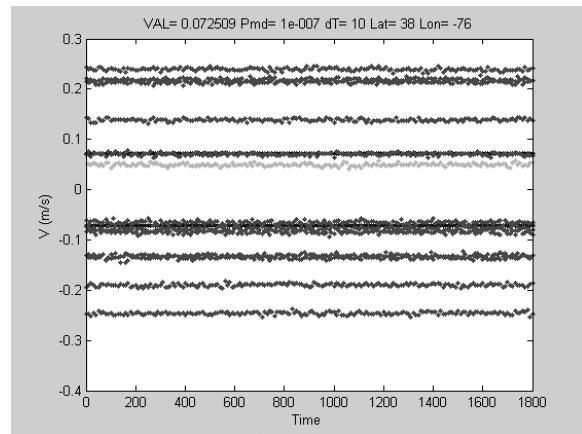


**Figure 9 Velocity Vertical Alarm Limits for HAL=1.3, VAL=2.0 and dT=10 (Grey marks undetected satellite failures, Black marks detected satellite failures)**

### KCPT Integrity Design

The purpose of the KCPT integrity monitoring test is to provide a confidence level for the ambiguity phase resolution of the kinematic GPS solution. If this is set correctly, then the KCPT position solution is accurate to the carrier phase noise, scaled by the solution geometry. If the carrier ambiguity is set incorrectly, then the KCPT solution is biased by the ambiguity error. In other research, the ambiguity resolution approach has been derived based on white, Gaussian measurement noise assumptions<sup>ix</sup>.

Under this effort actual measurement errors were evaluated under field test conditions to allow development of an ambiguity resolution

algorithm optimized for non-Gaussian, real-world error model assumptions.

The test data analyzed was collected from a GPS/inertial mobile test set using differential and kinematic corrections provided by a stationary reference receiver. The mobile and reference GPS receivers used were Novatel Millennium dual frequency (L1/L2) codeless receivers. The inertial measurement unit used was a Honeywell HG1700 RLG IMU. The integrated GPS/inertial solution was generated using our InterNav software<sup>x</sup>. Raw GPS measurement data was also collected for post-test analysis to evaluate the measurement quality for both the reference and the mobile receivers.

### Kinematic Solution Detection Tests

The following conditions must be in the Kinematic solution algorithm.

1. The starting inertial navigation solution must be within the search space ellipse for selecting the ambiguity space. To assure that we meet this condition, the search space ellipse must be set such that the probability of missed detection for the integrity solution is met. This is performed by setting the search ellipse based on the inertial predicted solution error from the Kalman Filter factored by a scale factor.
2. The selected ambiguity solution must have a confidence level also consistent with the probability of missed detection. If Gaussian noise assumptions were valid, then this could be derived solely based on the chi-square statistical test shown in equation 10. Since the noise is in fact highly correlated, a more robust detection test must be applied.
3. If cycle slips occur these must be detected and the ambiguity associated with this satellite recomputed. This can be achieved by using the RAIM test performed on the individual fault vectors which can identify cases where a cycle slip has occurred.

The test metric that we have determined to be most reliable in terms of identifying the correct integer ambiguity in the presence of correlated noise is based on equation 8. This selects the subset of valid ambiguity candidates based on

the members of the test set that pass the following threshold.

### Eq. 8)

$$F(t_{lock}, k) < \max\left(\frac{invchisq(1 - P_{MD}, N dof)}{N dof}, W_\alpha\right) \max(\hat{\sigma}_{CPH}^2 N dof, \min(F(t_{lock}, k)))$$

The estimate of the carrier phase noise is computed using a filtered noise estimate from the minimum fault vector ( $k_{min}$ ), as shown in equation 9.

### Eq. 9)

$$\hat{\sigma}_{CPH}^2 = \hat{\sigma}_{CPH}^2 (1 - K) + K f(t_{lock}, k_{min})^T f(t_{lock}, k_{min}) / (m - 3)$$

This provides an estimate of the 1-sigma noise on the measurements. If the noise were purely Gaussian then the correct ambiguity would pass the following test metric given in equation 10.

### Eq. 10)

$$F(t_{lock}, k) < \frac{invchisq(1 - P_{MD}, N dof)}{N dof} \hat{\sigma}_{CPH}^2 N dof = invchisq(1 - P_{MD}, N dof) \hat{\sigma}_{CPH}^2$$

If the noise is not Gaussian (which is the general case due to the presence of correlated multipath error), then the minimum value of F may not identify the correct ambiguity. The test that is used to isolate the correct ambiguity in this case is by comparing the minimum F value with the other members of the set. When the minimum value is distinguished from the other hypothesized value by a scale factor threshold ( $W_\alpha$ ) then the ambiguity solution is assumed to have converged.

An example of this selection method is shown in Figure 11. The initial ellipse search space and the GPS/INS Kalman filter derived position solution, compared with the “truth” kinematic solution is shown in Figure 10. This shows that the filtered GPS/inertial solution is effective at keeping the search space small for ambiguity resolution and provides a reliable starting condition to determine the ambiguity set.

For the mobile data set used to test this algorithm, the initial search space identified 100

possible ambiguities, and the correct ambiguity was resolved in less than 60 seconds.

In Figure 11 the set of F test metrics for the different ambiguity sets is shown over time. From this plot, it is easy to “eye-ball” that the correct value was indeed selected. By comparing the minimum and the next to minimum metrics associated with the hypothesized ambiguity sets, the correct set can be identified and the associated confidence level can also be estimated even though correlated errors are present. This Fault detection and isolation selection algorithm for identifying the correct ambiguity is the approach that will be implemented in future work.

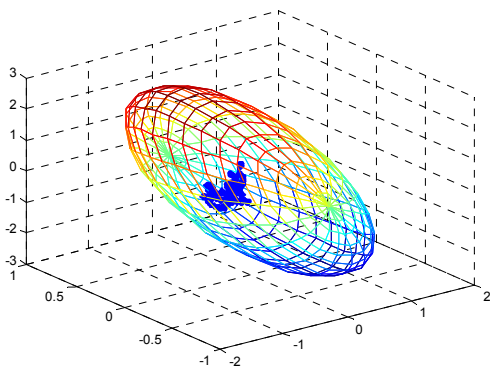


**Figure 10 GPS/INS Kalman Filter Position relative to KGPS solution**

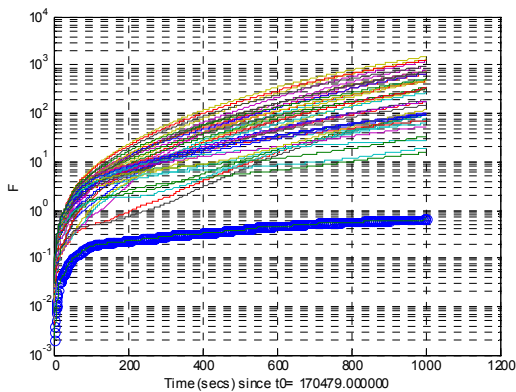


**Figure 11 FDI Detection metric (F) of correct ambiguity**

### High-gain Advanced GPS Receiver (HAGR)

To test these algorithms, we propose to develop an airborne configuration of our digital

beam/null-steering GPS receiver, the HAGR<sup>[xi]</sup>. The HAGR adopts a modular hardware architecture that allows it to be scaled based on the user’s desired configuration. An example configuration is shown in Figure 12.

Each HAGR includes the following subsystem elements. One or more Digital Front-End card(s) digitally sample the GPS RF signals, and all operate using common local oscillator signals and sample clocks provided by the local time generator and synthesizer module. One or more Digital Beam Steering Cards (DBS) combine the digitized antenna signals and provide 12 digital composite signal outputs. These are passed to the Correlation Acceleration Card (CAC) which performs the GPS signal correlation and tracking functions under control of the host computer. These cards are all installed in a Compact PCI back-plane.

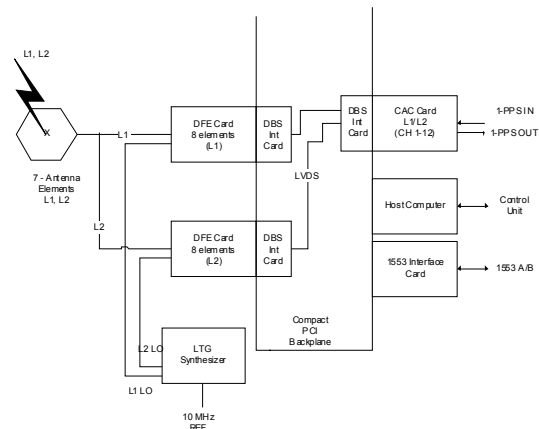


**Figure 12 A 7-element L1/L2 HAGR-A Configuration**

The proposed test-bed will be configured for integration onto a test aircraft installed with a standard CRPA antenna array. The HAGR system is to be installed into an aircraft ready ATR chassis, as shown in Figure 13.



**Figure 13 HAGR-A Receiver in ATR chassis**

### Concluding Observations

Based on the analysis performed under this effort, the following observations were drawn on the development of the hybrid integrity monitoring approach. Spatial Environment Integrity Monitoring will require special purpose firmware in the spatial and GPS signal processing to generate pre-correlation and post-correlation power matrices in order to detect the spatial signal and hardware failure modes identified. In order to achieve the desired HAL and VAL limits with the specified  $P_{MD}$  of  $10^{-7}$ , the GPS range-rate error must be monitored to assure that the inertial navigation error is not corrupted during the precision approach.

Based on the LN-100 error model, an optimum integrity monitoring time period for detecting small GPS range rate errors and bounding the possible velocity error that can be introduced, is 10 seconds. HAL and VAL limits of 1 meter can be achieved when there is sufficient integrity geometry available. To achieve a global availability of 99.8% for the integrity monitoring, the HAL and VAL limits have to be relaxed to 1.3 m and 2 m respectively, however HAL and VAL of 1 meter can be achieved at some locations. A more precise definition of availability is needed to provide a specific recommendation on the HAL and VAL limits that should be set for the integrity monitoring function. Non-Gaussian detection statistics must be assumed to perform reliable kinematic ambiguity resolution and assure the integrity of the kinematic solution.

### References

- <sup>i</sup> System makes historic flight for naval aviation, "<http://www.cnrma.navy.mil/news/june2001/2060701/2060701.html>"
- <sup>ii</sup> Lee, Young C. and D. G. O’Laughlin, “A Performance Analysis of a Tightly Coupled GPS/Inertial System for Two Integrity Monitoring Applications,”[http://www.mitre.org/work/tech\\_papers/tech\\_papers\\_00/lee\\_analysis/lee\\_analysis.pdf](http://www.mitre.org/work/tech_papers/tech_papers_00/lee_analysis/lee_analysis.pdf)”
- <sup>iii</sup> Gautier, J., “GPS/INS Generalized Evaluation Tool for the Design and Testing of Integrated Navigation System, PhD Thesis, Stanford Univ., June 2003.
- <sup>iv</sup> Brown, A and N. Gerein, NAVSYS Corporation, “Test Results of a Digital Beamforming GPS Receiver in a Jamming Environment”, Proceedings of ION GPS 2001, Salt Lake City, Sept 2001.
- <sup>v</sup> Kaplan, E.D, ed, “Understanding GPS Principles and Applications, Artech House Publishers, 1996.
- <sup>vi</sup> “GPS/IMU Ultra-Tightly Coupled Integrity Monitoring Final Report,” NAVSYS Document No. GI-RAIM 02- 016, February 7, 2002
- <sup>vii</sup> R. Douglas, “A GPS Signal Residual Estimator for Ultra-Tight Receivers,” The Aerospace Corporation, October 2000
- <sup>viii</sup> “Autonomous Failure Detection for Differential GPS,” NAVSYS Document USCG 95-12.
- <sup>ix</sup> Teunissen, P.J.G., P.J. de Jonge, and C.C.J.M. Tiberius (1996) “The volume of the GPS ambiguity search space and its relevance for integer ambiguity resolution”. Proceedings of ION GPS-96, 9th International Technical Meeting of the Satellite Division of the Institute of Navigation, Kansas City, Missouri, Sept. 17-20, pp. 889-898.
- <sup>x</sup> <http://www.navsys.com/Products/internav.htm>
- <sup>xi</sup> <http://www.navsys.com/Products/hagr.htm>

### Acknowledgements

The authors gratefully acknowledge the U.S. Navy’s Naval Air Warfare Center for supporting this research. However, the views expressed in this paper belong to the authors alone and do not necessarily represent the position of any other organization or person.